American Mineralogist, Volume 94, pages 981–985, 2009

Polarized infrared spectroscopic study of diffusion of water molecules along structure channels in beryl

Junichi Fukuda,[1,*] Keiji Shinoda,[2] Satoru Nakashima,[1] Naoya Miyoshi,[2] and Nobuyuki Aikawa[2]

[1]Department of Earth and Space Science, Graduate School of Science, Osaka University 1-1 Machikaneyama, Toyonaka, Osaka 560-0043, Japan
[2]Department of Geosciences, Graduate School of Science, Osaka City University 3-3-138 Sugimoto, Sumiyoshi, Osaka 558-8585, Japan

Abstract

Incorporation of water in anhydrous synthetic beryl was studied at 500–700 °C and 50–150 MPa of confining water pressure to measure the diffusion of water molecules along the channels in a cyclosilicate. A series of polarized IR spectra series were taken with **E** parallel to the channel direction, which is parallel to the *c*-axis, along a traverse parallel to this axis. Water concentration profiles were determined from absorbance of H_2O peaks. The IR spectra showed that the dominant diffusing species is type I water molecule, whose H-H vector is parallel to the *c*-axis (sharp peak at 3700 cm^{-1}). No pressure dependence on water diffusivity can be recognized under these experimental conditions. The Arrhenius relation gives the activation energy of 133 ± 12 kJ/mol, with a pre-exponential factor of $10^{-2.6}$ (cm^2/s). Diffusion of water is much faster in the beryl channels than volume diffusion in other silicates, but the activation energy and diffusion coefficient values for beryl are similar to the corresponding values previously reported for grain boundary diffusion in quartz aggregates.

Keywords: Water molecule, cyclosilicate, beryl channels, fast diffusion, IR spectroscopy

Introduction

The diffusivities of H_2O, H^+, and H_3O^+ have been widely studied for minerals in both single crystals and polycrystalline aggregates because of their importance in the Earth and material sciences (summarized in Brady 1995; Watson and Baxter 2007). Three diffusional processes are recognized: volume (intracrystalline) diffusion, dislocation or pipe diffusion, and grain boundary diffusion. Volume diffusion in a crystal is generally much slower than diffusion through high diffusivity paths such as dislocations and grain boundaries. Long and narrow structural cavities called channels are characteristic of cyclosilicate structures such as beryl and cordierite. Since these channels are not crystal defects, diffusion of water through them should be via volume diffusion. However, diffusion through the channels may be more likely due to mobility along high diffusivity paths because atoms in the crystal structure do not impede the diffusion of water molecules when the channels are empty. Water diffusivities have been reported for several silicates [Farver and Yund (1991a) for α-quartz, Fortier and Giletti (1991) for mica, Goryainov and Belitsky (1995) for zeolite, and Demouchy and Mackwell (2003) for forsterite], but only a few experimental studies have been conducted on rapid volume diffusion of water through crystal structures with channels. Most diffusion experiments of water in minerals have used isotopes such as ^{18}O and D and determined the concentration profile of the isotope by ion-microprobe analysis or the bulk concentration of diffused isotope by mass spectroscopy. This approach determines only the concentration of the particular isotope. It is also difficult to understand the interaction between diffusing species and the crystal structure without structural information during the diffusion process.

Beryl is a typical cyclosilicate and its structure comprises hexagonal rings of corner-shared SiO_4 tetrahedra. The stacking of six tetrahedra forms a pipe-like cavity along the crystallographic *c*-axis known as a channel (Gibbs et al. 1968). A channel is composed of alternating larger and smaller cages at the 2a and 2b positions, respectively. The cages are ~0.51 and 0.28 nm across and are surrounded by oxygen atoms. Beryl is a nominally anhydrous mineral, but extra-framework water molecules are often incorporated in the channels of natural beryl. Two types of water molecule, referred to as type I and type II, are located at 2a position (Wood and Nassau 1967). Type I is oriented with the H-H vector parallel to the *c*-axis. When an extra-framework cation is located at 2b position, a water molecule bonds to the cation by electric force between the cation and a water molecule and its H-H vector is perpendicular to the *c*-axis. Extra-framework cations are incorporated to maintain charge balance for replacement of Be^{2+} by Li^+ or Al^{3+} by Fe^{2+} (Hawthorne and Černý 1977; Aurisicchio et al. 1988). Many spectroscopic studies have been performed to investigate the state of water molecules in the beryl channels since the publication by Wood and Nassau (1967), which gave strong evidence for the two types of water molecules as described above. On the basis of a polarized infrared (IR) spectroscopic study of hydrated synthetic beryl and dehydrated natural beryl, Fukuda and Shinoda (2008) proposed that there are small vibrational energy gaps between type II water molecules coordinated to a single extra-framework cation and type II water molecules coordinated to two such cations.

Water and carbon dioxide contents of beryl under various temperature and pressure conditions have been studied as po-

* E-mail: jfukuda@ess.sci.osaka-u.ac.jp

tential fugacity indicators (Pankrath and Langer 2002) as have those of cordierite, which is a cyclosilicate structurally similar to beryl. Water and carbon dioxide diffusion experiments for cordierite were performed and their maximum contents were reported by Johannes and Schreyer (1981). However, diffusion mechanisms through channels in beryl and cordierite are still not well understood.

In this study, we investigated diffusion of water molecules in beryl channels by polarized IR spectroscopy and have compared the diffusion coefficients for water molecules and the activation energy in beryl with those of water in other materials for which data are available.

Experimental methods

Anhydrous beryl was synthesized from Li_2CO_3-MoO_3 flux (Oishi 1994; Oishi and Mochizuki 1995). Average contents of major elements over 0.05 wt% as oxides are 64.89 wt% SiO_2, 18.60 wt% Al_2O_3, 14.07 wt% BeO, 0.12 wt% FeO, 0.064 wt% TiO_2, 0.051 wt% Li_2O, and 3.01 wt% Na_2O (Fukuda and Shinoda 2008). Sodium content is relatively high and can be present as Na^+ in beryl channels (Hawthorne and Černý 1977; Aurisicchio et al. 1988). Some synthetic beryl crystals exhibited a cloudy part especially in the core, but only relatively transparent samples were selected for hydrothermal experiments. Several synthetic beryl crystals, about 1.5–2.0 mm long (*c*-axis direction), were enclosed in a gold capsule with 5–15 μL of water. Gold capsules were welded and placed into a hydrothermal vessel. Hydrothermal annealing experiments were performed at temperatures of 500–700 ± 1 °C under confining water pressures of 50, 100, and 150 ± 3 MPa, from 30 to 480 h (20 days) (Table 1). The recovered gold capsules sometimes showed an increase in weight of up to 2%. In these cases, we suspect that the water as a pressure medium of the hydrothermal vessel penetrated the gold capsule through imperfections no wider than pinholes in the jacket welds. The crystals in these gold capsules were always transformed into phases other than beryl, which were identified as chrysoberyl and phenakite by X-ray diffraction. The following reaction between beryl and large amounts of water as described by Barton (1986) can explain the above transformation:

$$2Be_3Al_2Si_6O_{18} + 14H_2O \rightarrow 3Be_2SiO_4 + 2Al_2SiO_5 + 7H_4SiO_4.$$

The recovered samples without the weight increase were polished into plates 60–100 μm thick, parallel to the *c*-axis. Polarized IR absorption spectra of the thin sections were measured with **E** (the electric vector of IR light) parallel to the *c*-axis using a Fourier transform infrared (FTIR) microspectrometer (Shimadzu FTIR4200 with an IR microscope IMS-1), equipped with a ceramic light source, a KBr beam splitter and a MCT detector (Shinoda and Aikawa 1993). IR spectra were obtained by scanning 512 times with a wavenumber resolution of 2 cm^{-1}. A series of sample spectra were obtained by measuring polarized IR spectra along the *c*-axis with an aperture of 50 μm from rim to core of the thin sections in steps of 10 to 20 μm. Although some diffusional water uptake was observed perpendicular to the *c*-axis, it can be neglected compared with the diffusional uptake parallel to the *c*-axis.

Results

A representative series of polarized IR spectra for synthetic beryl obtained at different distances from the rim along the *c*-axis are shown in Figure 1a for regions of water stretching and bending vibrations. A band at 3700 cm^{-1} is prominent, and this peak is due to ν_3 mode of type I water molecule (after Wood and Nassau 1967). However, doublet ν_1 and ν_2 modes of type II water molecule were occasionally recognized at 3602 and 3589 cm^{-1}, and 1631 and 1619 cm^{-1}, respectively as shown in Figure 1b. Our previous study (Fukuda and Shinoda 2008) suggests that the bands at 3602 and 1619 cm^{-1} could be assigned to two type II water molecules coordinated to a cation (Na^+), and those at 3589 and 1631 cm^{-1} to one type II water molecule coordinated to Na^+. The absorption intensities of doubly coordinated type II water molecules become larger than those of singly coordinated

Table 1. Conditions of hydrothermal experiments

P (MPa)	Fugacity (MPa)	*T* (°C)	Duration (h)	Log D (cm^2/s)
50	31	500	360	−11.46
50	38	600	240	−10.74
50	43	700	48	−9.40
100	45	500	480	−11.37
100	54	550	312	−11.06
100	62	600	168	−10.78
100	69	650	93	−10.33
100	76	700	36	−9.56
150	56	500	360	−11.47
150	81	600	168	−10.74
150	122	700	30	−9.61

Note: The errors of diffusion coefficients were within 2%.

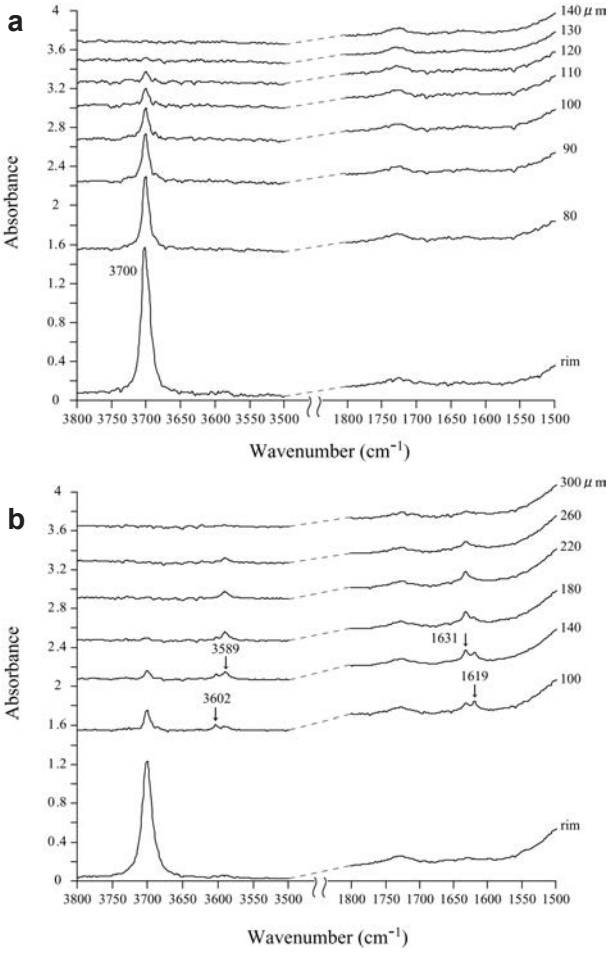

Figure 1. (**a**) Polarized IR spectra (**E**//*c*-axis) of hydrated synthetic beryl in the regions of water stretching and bending modes. The depth from the rim is shown on the right. The anhydrous sample was hydrothermally hydrated at 650 °C and 100 MPa for 93 h. Only the 3700 cm^{-1} band due to ν_3 mode of type I water molecule can be observed (cf. **b**). (**b**) Polarized IR spectra (**E**//*c*-axis) of hydrated synthetic beryl in the regions of water stretching and bending modes. The depth from the rim is shown on the right. The anhydrous sample was hydrothermally hydrated at 700 °C and 150 MPa for 30 h. In addition to the ν_3 mode of type I water molecule at 3700 cm^{-1} (cf. **a**), doublet bands at 3602 and 3589 cm^{-1} due to ν_2 modes and 1631 and 1619 cm^{-1} of type II water molecules are observed. These doublet bands are thought to originate from different coordination numbers of type II water molecule to a cation (Na^+) (Fukuda and Shinoda 2008).

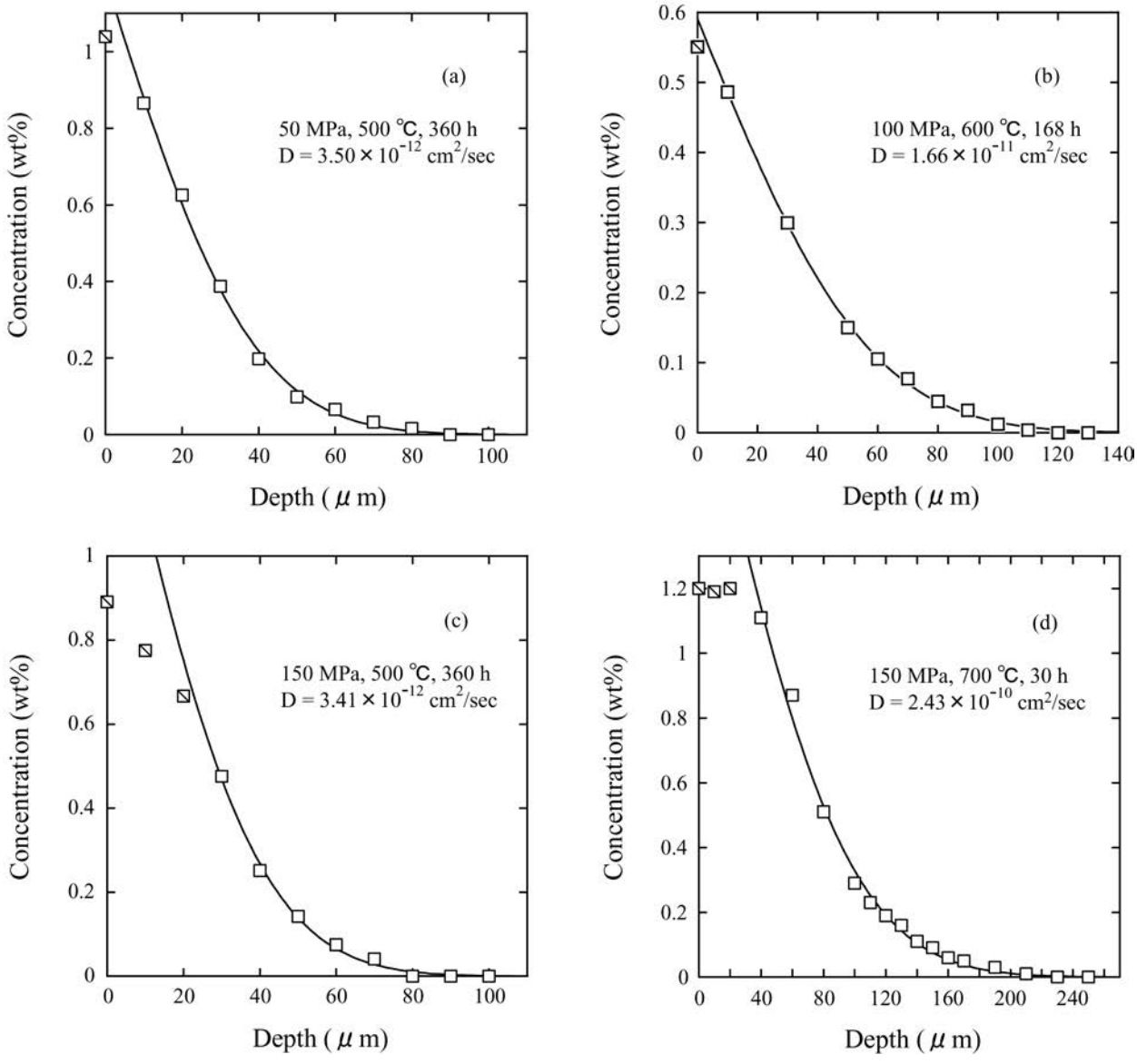

FIGURE 2. Water concentration profiles (open squares) vs. the depth from the sample surface. Each concentration was determined from absorbance of water IR bands (see text for explanation). The experimental data are fitted by the diffusion model (Eq. 2 in text: solid curves) except for the data near the rim shown as squares with one diagonal (see text for explanation). Diffusion coefficients are given with experimental temperatures and pressures.

type II at positions closer to the sample rim (Fig. 1b). The intensity ratio of doubly coordinated type II water relative to singly coordinated type II water increased because of the increase in total water content.

The water content was calculated from Lambert-Beer's law:

$$A = \varepsilon C d \quad (1)$$

where A is the absorbance (peak height), ε is the molar absorption coefficient (L/mol·cm), C is the concentration of water (mol/L), and d is the thickness of the sample (cm). The molar absorption coefficient of ν_3 mode of type I water molecule, (197 L/mol·cm) determined by Charoy et al. (1996) was used for the calculation. Since the absorption coefficient of ν_1 mode of type II water for beryl is not yet known, that of the same mode for cordierite determined by Goldman et al. (1977) (256 L/mol·cm) was adopted for the calculation (Aines and Rossman 1984). Since the maximum absorbance of type II water is 0.1 corresponding to only 0.05 wt% water assuming an 80 μm sample thickness, the bulk concentration of water mainly depends on the amount of type I water (up to 1 wt%). Thus, the total concentration of water, including types I and II, was determined over the length of the crystal. Representative water concentration profiles are shown in Figure 2.

The water concentration profiles (Fig. 2) were fitted by the solution of a simple one dimensional diffusion equation as follows (Crank 1975, p. 21):

$$C = C_0 erfc\left(\frac{x}{2\sqrt{Dt}}\right) \quad (2)$$

where C is the concentration at depth x (cm) from the sample rim; C_0 is the maximum concentration; D is the diffusion coefficient (cm^2/s); t is the time duration (s); and *erfc* is the complementary error function. All concentration profiles were fitted by the above equation except for the first 20 μm from the sample rims (Fig. 2). The resulting curves gave good results and similar diffusion coefficients at the same temperature for crystal interiors (e.g., Figs. 2a and 2c). The diffusion coefficients determined from the above equation for the crystals (excluding rims) are listed in Table 1 and discussed in the next section. Water contents of beryl measured along traverses perpendicular to the *c*-axis were two orders of magnitude less than those determined along traverses parallel to the *c*-axis. Thus, diffusion perpendicular to the *c*-axis was neglected in this study.

Deviations from diffusion curves at the rims are different in each sample. They do not depend on the water concentration or water diffusion depth (compare Fig. 2d and others). In their study of zeolite, Goryainov and Belitsky (1995) also reported deviations in water contents from the diffusion profiles near the rim. There is no obvious explanation for the deviations, but one possibility is structural heterogeneity near the surface of the sample.

Figure 3 shows the Arrhenius diagram for diffusion coefficients obtained at 500–700 °C and under 50–150 MPa. All the data at different pressures were best fit by the following Arrhenius relation:

$$D = 10^{-2.6} \exp\left(-\frac{133 \pm 12 \text{kJ/mol}}{RT}\right) \quad (3)$$

where R is the gas constant and T is the absolute temperature. The pre-exponential factor is $10^{-2.6}$ cm^2/s and the activation energy is 133 ± 12 kJ/mol.

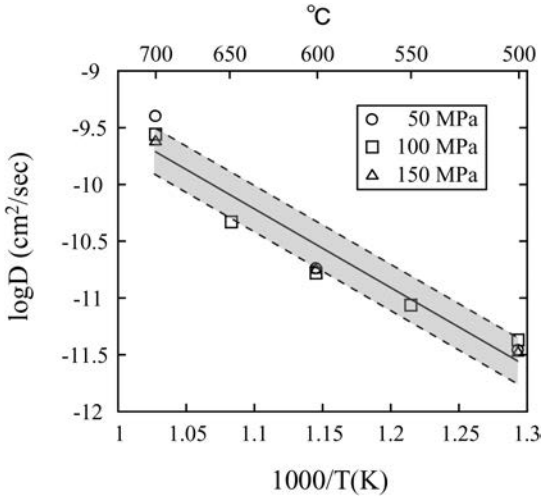

Figure 3. Arrhenius plot for diffusion coefficients of water in the beryl channels (parallel to the *c*-axis) obtained from the present authors' hydrothermal experiments at 500–700 °C under confining water pressures of 50, 100, and 150 MPa. Fitting of all the data by the Arrhenius equation gives the best fit (solid line) with errors (gray zone between dotted lines) and an activation energy of 133 ± 12 kJ/mol.

Discussion

In this study, the diffusing species in the channels are water molecules mainly in the form of type I water (OH peak at 3700 cm^{-1}), as can be seen in Figure 1. No significant pressure effects on water diffusion in beryl channels were observed in the experimental pressure range of 50–150 MPa (Fig. 3 and Table 1).

Diffusion coefficients and activation energy obtained in this study and those for other silicates including quartz grain aggregates (novaculite) are shown in Figure 4. The experimental conditions for the other studies are summarized in Table 2, in which the diffusing species inferred by authors are listed and the measured constituents shown as italics. Pressure ranges for these experiments are similar to those of the present study (100 to 200 MPa, except one study was done under vacuum).

Diffusion coefficients and activation energies of water in silicates are expected to be related to their structures. It is generally accepted that with more compact structures of silicates, diffusion coefficients become smaller and activation energies become larger. For example, SiO_4 tetrahedra of quartz share the corner O atoms and form channels along the *c*-axis. As the crystal structure of quartz is compact, quartz channels are not as open as beryl channels, and not surprisingly, diffusion coefficients and activation energy are smaller in both α-quartz and β-quartz than in beryl (Fig. 4). In the case of sheet silicates such as biotite, water is inferred to diffuse parallel to the layers through the interlayer spaces (Fortier and Giletti 1991). In the interlayer spaces of biotite, cations bind two neighboring layers. The bonding force between two neighboring layers is not as strong as the covalent bond of quartz. The interlayer spaces of biotite are not as compact as the quartz structure. Therefore, water must diffuse faster in biotite than in quartz. On the other hand, extrapolating the Arrhenius relation to our experimental temperature range,

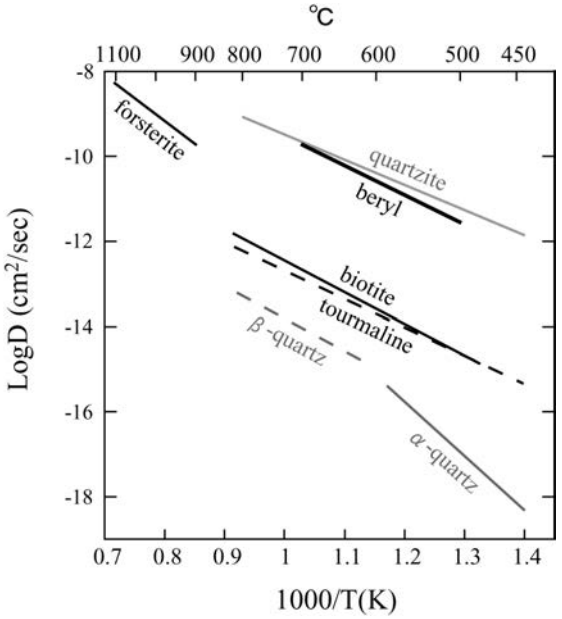

Figure 4. Arrhenius diagram of water diffusivities for various silicates. Beryl (this study) shows larger diffusivity than any other mineral in single crystals, and is similar to grain boundary water diffusion in quartzite (coarse quartz aggregates, novaculite). Numerical values and references for data from the literature are listed in Table 2.

TABLE 2. Summary of experimental data for water diffusion in various materials

Material	Diffusive direction	Diffusing species	*T* (°C)	*P* (MPa)	Activation energy (kJ/mol)	Log D_0 (cm^2/s)	Experiment + Measurement	Reference
α-quartz	//*c*-axis	$H_2{}^{18}O$	450–590	100	243	−0.5	$H_2{}^{18}O$ doping + ion probe	Farver and Yund (1991a)
β-quartz	//*c*-axis	$H_2{}^{18}O$	600–800	100	142	−6.4	$H_2{}^{18}O$ doping + ion probe	Giletti and Yund (1984)
biotite	⊥*c*-axis	$H_2{}^{18}O$	500–800	100	143	−5.0	$H_2{}^{18}O$ doping + ion probe	Fortier and Giletti (1991)
tourmaline	?	*D*	450–800	vacuum	128	−6.0	D_2O doping + Mass	Jibao and Yaqian (1997)
forsterite	⊥*c*-axis	vacancy + *H*	900–1110	200	205	−0.6	Pure H_2O doping + IR	Demouchy and Mackwell (2003)
quartzite	–	$H_2{}^{18}O$	450–800	100	113	−3.6	$H_2{}^{18}O$ doping + ion probe	Farver and Yund (1991b)

Notes: The diffusing species inferred by authors are listed. Elements directly measured in each experiment are shown as italics.

diffusion coefficients of water in forsterite are relatively large (Demouchy and Mackwell 2003) in spite of the compact crystal structure. Although their diffusion experiment was performed using H_2O, Demouchy and Mackwell (2003) suggested that hydrogen diffuses as H^+ via vacancies in the forsterite crystal structure. The size and weight of H^+ as a diffusing species is much smaller than H_2O, diffusion coefficients of H^+ in forsterite are larger than the diffusion coefficients of H_2O in other silicates. In the diffusion experiments of tourmaline conducted under D_2O-saturated conditions, the diffusing species was assumed to be D^+. Tourmaline is a cyclosilicate and stoichiometrically includes OH^-. Therefore, D^+ must diffuse via the proton sites (Jibao and Yaqian 1997). While smaller D^+ would diffuse faster than larger H_2O in tourmaline, the diffusivity of D^+ must be lowered in the compact crystal structure of tourmaline. In beryl channels, the IR spectra showed that large H_2O diffuses through the channels. In our experimental temperature range, the diffusion coefficients of H_2O in beryl channels are approximately three orders of magnitude higher than those of D^+ in the compact crystal structure of tourmaline. This difference indicates that the compactness of the crystal structure is a dominant factor governing diffusion, and that beryl channels are sufficiently large for H_2O diffusion and lead to high diffusivity.

Interestingly, the diffusivity of water molecules in beryl channels is similar to that along grain boundaries, as determined for quartz aggregates by Farver and Yund (1991b). They calculated grain boundary diffusion coefficients for what were inferred to be water molecules (Table 2) from bulk diffusion measurements of oxygen under hydrothermal conditions. It is predicted that negatively charged oxygen atoms would be exposed at the surface of grains of silicates including quartz because Si-O bonds have been broken. In general, microstructures of grain surfaces are complex and gaps between grains are variable; Farver and Yund (1991b) assumed the surfaces in the quartz aggregates to be planar and separated by gaps as thin as 1 nm. Beryl channels are composed of cages 0.51 and 0.28 nm in diameter bound by negatively charged oxygen atoms, i.e., roughly the same size as the gaps between grains in the quartz aggregates, and also bound by negative charges. That the diffusion coefficients and activation energy of water diffusion through the channels in beryl are similar to corresponding parameters for diffusion along grain boundaries in quartz aggregates attests to the similarity in environments for the diffusing water molecules in these otherwise very dissimilar materials.

ACKNOWLEDGMENTS

The authors thank H. Masuda and M. Katsura for their valuable discussion and comments as well as all members of Department of Earth and Space Science, Osaka University, and Department of Geosciences, Osaka City University, for their suggestions and continuous encouragement. A. Kronenberg and G. Rossman are also thanked for their official and constructive reviews as well as E. Grew for editorial handling and his kind review. The IR absorption spectra were partly measured at the BL43IR in the SPring-8 with the approval of the Japan Synchrotron Radiation Research Institute (JASRI) (proposal no. 2006A1768).

REFERENCES CITED

Aines, R.D. and Rossman, G.R. (1984) The high temperature behavior of water and carbon dioxide in cordierite and beryl. American Mineralogist, 69, 319–327.

Aurisicchio, C., Fioravanti, G., Grubessi, O., and Zanazzi, P.F. (1988) Reappraisal of the crystal chemistry of beryl. American Mineralogist, 73, 826–837.

Barton, M.D. (1986) Phase equilibria and thermodynamic properties of minerals in the BeO-Al_2O_3-SiO_2-H_2O (BASH) system, with petrologic applications. American Mineralogist, 71, 277–300.

Brady, J.B. (1995) Diffusion data for silicate minerals, glasses, and liquids. In T.J. Ahrens, Ed., Mineral Physics and Crystallography: A Handbook of Physical Constants, 2, p. 269–290. American Geophysical Union Reference Shelf, AGU, Washington, D.C.

Charoy, B., de Donato, P., Barres, O., and Pinto-Coelho, C. (1996) Channel occupancy in an alkali-poor beryl from Serra Branca (Goias, Brazil): Spectroscopic characterization. American Mineralogist, 81, 395–403.

Crank, J. (1975) The Mathematics of Diffusion, 2nd edition, p. 21. Oxford University Press, New York.

Demouchy, S. and Mackwell, S. (2003) Water diffusion in synthetic iron-free forsterite. Physics and Chemistry of Minerals, 30, 486–494.

Farver, J.R. and Yund, R.A. (1991a) Oxygen diffusion in quartz: Dependence on temperature and water fugacity. Chemical Geology, 90, 55–70.

——— (1991b) Measurement of oxygen grain boundary diffusion in natural, fine-grained, and quartz aggregates. Geochimica et Cosmochimica Acta, 55, 1597–1607.

Fortier, S.M. and Giletti, B.J. (1991) Volume self-diffusion of oxygen in biotite, muscovite, and phlogopite micas. Geochimica et Cosmochimica Acta, 55, 1319–1330.

Fukuda, J. and Shinoda, K. (2008) Coordination of water molecules with Na^+ cations in beryl channel as determined by polarized IR spectroscopy. Physics and Chemistry of Minerals, 35, 347–357.

Gibbs, G.V., Breck, D.W., and Meagher, E.P. (1968) Structural refinement of hydrous and anhydrous synthetic beryl, $Al_2(Be_3Si_6)O_{18}$ and emerald, $Al_{1.9}Cr_{0.1}(Be_3Si_6)O_{18}$. Lithos, 1, 275–285.

Giletti, B.J. and Yund, R.A. (1984) Oxygen diffusion in quartz. Journal of Geophysical Research, 89, 4039–4046.

Goldman, D.S. and Rossman, G.R. (1977) Channel constituents in cordierite. American Minralogist, 62, 1144–1157.

Goryainov, S.V. and Belitsky, I.A. (1995) Raman spectroscopy of water tracer diffusion in zeolite single crystals. Physics and Chemistry of Minerals, 22, 443–452.

Hawthorne, F.C. and Černý, P. (1977) The alkali-metal positions in Cs-Li beryl. Canadian Mineralogist, 15, 414–421.

Jibao, G. and Yaqian, Q. (1997) Hydrogen isotope fractionation and hydrogen diffusion in the tourmaline-water system. Geochimica et Cosmochimica Acta, 61, 4679–4688.

Johannes, W. and Schreyer, W. (1981) Experimental introduction of CO_2 and H_2O into Mg-cordierite. American Journal of Science, 281, 299–317.

Oishi, S. (1994) A simple method of growing emerald crystals. Ceramics, 29, 417–420.

Oishi, S. and Mochizuki, K. (1995) Growth of emerald crystals by the flux evaporation method in Li_2O-MoO_3 flux. Journal of Materials Chemistry, 5, 1257–1260.

Pankrath, R. and Langer, K. (2002) Molecular water in beryl, $^{VI}Al_2[Be_3Si_6O_{18}]\cdot nH_2O$, as a function of pressure and temperature: An experimental study. American Mineralogist, 87, 238–244.

Shinoda, K. and Aikawa, N. (1993) Polarized infrared absorbance spectra of an optically anisotropic crystal: Application to the orientation of the OH^- dipole in quartz. Physics and Chemistry of Minerals, 20, 308–314.

Watson, E.B. and Baxter, E.F. (2007) Diffusion in solid-Earth systems. Earth and Planetary Science Letters, 253, 307–327.

Wood, D.L. and Nassau, K. (1967) Infrared spectra of foreign molecules in beryl. Journal of Chemical Physics, 47, 2220–2228.

MANUSCRIPT RECEIVED OCTOBER 20, 2008
MANUSCRIPT ACCEPTED FEBRUARY 26, 2009
MANUSCRIPT HANDLED BY EDWARD GREW